

# ST-LoRA: Low-rank Adaptation for Spatio-Temporal Forecasting

Weilin Ruan<sup>\*1,2</sup>, Wei Chen<sup>\*1</sup>, Xilin Dang<sup>3</sup>, Jianxiang Zhou<sup>1</sup>,  
Weichuang Li<sup>1</sup>, Xu Liu<sup>4</sup>, and Yuxuan Liang<sup>1</sup> (✉)

<sup>1</sup> The Hong Kong University of Science and Technology (Guangzhou), China  
onedeancxx@gmail.com, wli043@connect.hkust-gz.edu.cn, yuxiang@outlook.com

<sup>2</sup> Jinan University, Guangzhou, China rwlinno@gmail.com

<sup>3</sup> The Chinese University of Hong Kong, Hongkong xldang23@cse.cuhk.edu.hk

<sup>4</sup> National University of Singapore, Singapore liuxu@comp.nus.edu.sg

**Abstract.** Spatio-temporal forecasting is crucial in real-world dynamic systems, predicting future changes using historical data from diverse locations. Existing methods often prioritize the development of intricate neural networks to capture the complex dependencies of the data, yet their accuracy fails to show sustained improvement. Besides, these methods also overlook node heterogeneity, hindering customized prediction modules from handling diverse regional nodes effectively. In this paper, our goal is not to propose a new model but to present a novel **low-rank** adaptation framework as an off-the-shelf plugin for existing spatial-temporal prediction models, termed **ST-LoRA**, which alleviates the aforementioned problems through node-level adjustments. Specifically, we first tailor a node adaptive low-rank layer comprising multiple trainable low-rank matrices. Additionally, we devise a multi-layer residual fusion stacking module, injecting the low-rank adapters into predictor modules of various models. Across six real-world traffic datasets and six different types of spatio-temporal prediction models, our approach minimally increases the parameters and training time of the original models by less than 4%, still achieving consistent and sustained performance enhancement.

**Keywords:** Spatio-temporal forecasting · Low-rank Adaptation

## 1 Introduction

With the rapid development of data acquisition technologies and mobile computing, large amounts of spatio-temporal data are generated for urban analysis and related applications [7]. Spatio-temporal forecasting aims to predict future changes based on the dynamic temporal observations recorded at static locations with spatial associations. Modeling and analyzing this spatio-temporal dynamic system can be applied to various spatio-temporal prediction scenarios, such as

---

<sup>\*</sup> The first two authors contributed equally to this work.

traffic speed forecasting [31,29], taxi demand prediction [30], and air quality prediction [15,17].

Early efforts focused on traditional time-series models, such as vector auto-regression model [34] and autoregressive integrated moving average model [4]. These methods were directly applied to spatio-temporal forecasting tasks without considering spatial dependencies, resulting in poor performance. Leveraging collected spatio-temporal big data, recent approaches have shifted towards data-driven deep learning models, attributed to their capability to capture inherent spatio-temporal dependencies within dynamic systems. Simple ideas include using convolutional neural networks (CNNs) for spatial dependency capture and recurrent neural networks (RNNs) for temporal dependency capture, yielding performance improvements [6]. Considering the non-Euclidean nature of spatial dependencies, spatio-temporal graph neural networks (STGNNs) have gained significant attention due to their ability to learn robust high-level spatio-temporal representations through local information aggregation [10]. Recently, many advanced frameworks have attempted to leverage Self-Supervised Learning [24] and Large Language Models [33] techniques into spatio-temporal predicting tasks with improved performance. *However, the integration of these techniques often comes at the cost of increased computational complexity and memory requirements, making it challenging to achieve significant performance improvements without sacrificing efficiency.*

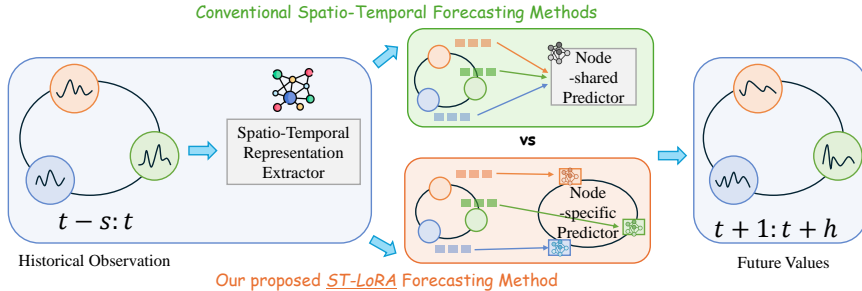


Fig. 1: Conventional forecasting methods vs. our ST-LoRA.

In light of this, we aim to summarize and analyze the architectures of existing methods, providing different insights. Specifically, existing spatio-temporal forecasting methods typically consist of two main components, as illustrated in Figure 1(a). The first component is the *Spatio-Temporal Representation Extractor*, which serves as the core framework and is responsible for capturing high-order complex spatio-temporal relationships. This component can be implemented using various architectures, such as convolutional neural networks (CNNs), RNNs, and STGNNs. The second component is the *Node-shared Predictor*, which takes the advanced spatio-temporal representations extracted by the first component and predicts future changes for each location. This predictor typically consists of parameter-sharing fully connected layers. While this two-component architecture has been widely adopted in existing methods, it suffers from a significant limitation. The parameter-sharing node predictor often fails to effectively model

the heterogeneous characteristics of individual nodes. In other words, the predictor assumes that all nodes exhibit similar behavior and can be modeled using the same set of parameters. *However, in real-world scenarios, different nodes may have distinct patterns and dynamics, which cannot be captured by a shared predictor.*

To illustrate this problem intuitively, we provide a simple example. As shown in Figure 2, on the left is the state of California where the PEMS04 traffic flow dataset [5] is located. We select three groups of nodes, each in a different area: commercial, educational, and residential zones. Visualizing the traffic flow changes over a period for each group of nodes, we observe starkly different variations in traffic flow among the different areas. Particularly, the residential area exhibits significantly lower traffic flow due to its residential function. Moreover, even within the residential area, nodes 33 and 93 show noticeable changes from time steps 1750 to 2000, likely due to their proximity to the commercial zone. Consequently, existing methods, which rely solely on parameter-sharing node predictors, struggle to capture the diverse distribution changes among different nodes over time, resulting in limited prediction performance.

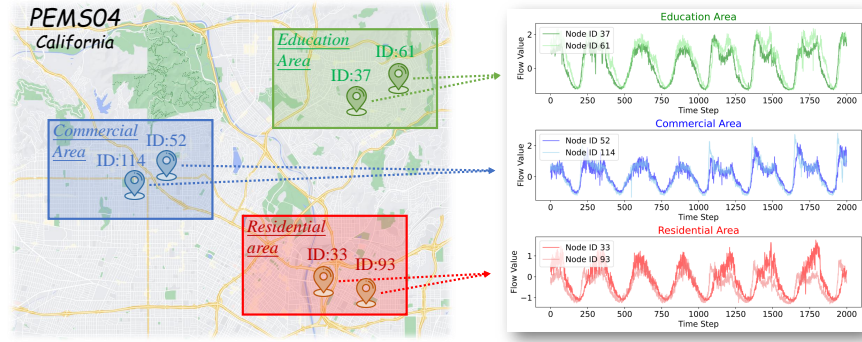


Fig. 2: Traffic flow visualization of each node in different areas on the PEMS04.

Upon reexamining existing methods and potential reasons, we argue that the critical factor undermining spatio-temporal forecasting lies in the insufficient generalization capability of the generic node predictors used by most prediction models to address diverse spatio-temporal heterogeneities. Hence, it is necessary to design a universal framework to address the above problem. However, due to the potentially massive number of nodes in spatio-temporal graphs, this is not simple, considering the following two reasons. Firstly, associating learning parameters with each node may significantly increase time costs and efficiency, necessitating a trade-off between performance and cost. Secondly, the massive parameters may lead to overparameterization, causing them to overfit noise information in the training data, resulting in suboptimal generalization.

To address the aforementioned challenges, we draw inspiration from low-rank matrix factorization techniques [23] and propose a novel lightweight and efficient low-rank adaptation framework, named ST-LoRA. This framework seamlessly

integrates into existing spatio-temporal forecasting models with minimal alteration to their core architectures by modifying only the node predictor module. Specifically, we first customize a node-adaptive low-rank layer containing multiple trainable matrices, leveraging low-rank decomposition techniques to effectively reduce computational complexity and enhance model training efficiency. Additionally, we design a multi-layer fusion residual stacking module to effectively inject the node-adaptive low-rank layer adaptation into the predictor modules of various models, thereby mitigating the effects of overparameterization. Experimental results on six real-world traffic datasets show that our framework significantly improves various baseline methods in spatio-temporal forecasting tasks. Our major contributions can be summarized as follows:

- *A node heterogeneity perspective for spatio-temporal forecasting.* We propose a novel approach that takes into account the heterogeneity of nodes in spatio-temporal networks. Our proposed module, termed Node Adaptive Low-rank Layer (NALL), leverages additional parameter space to capture the diverse characteristics and distributions of individual nodes. By employing low-rank matrix factorization techniques, NALL effectively captures the complex functional properties of each node while maintaining computational efficiency.
- *A general low-rank adaptation method for existing models.* We design a framework called ST-LoRA that can pass in a spatio-temporal forecasting model as a backbone and assemble a residual fusion module, which contains multiple NALLs and tuning modules to improve performance.
- *Extensive empirical studies.* We evaluate our proposed method on different models and six public traffic datasets. The results affirm that our method enhances original models and possesses superior generalization ability. The source code is publicly available: <https://github.com/RWLInno/ST-LoRA>

## 2 Preliminaries

### 2.1 Formulation

The objective of spatio-temporal forecasting is to predict future values based on previously observed time series data from  $N$  correlated sensors. This sensor network can be represented as a weighted directed graph  $\mathcal{G} = (\mathcal{V}, \mathcal{E}, \mathcal{W})$ , where  $\mathcal{V}$  is the node set with  $|\mathcal{V}| = N$ ,  $\mathcal{E}$  is the edge set, and  $\mathcal{W} \in \mathbb{R}^{N \times N}$  is a weighted adjacency matrix that encodes the relationships between nodes. The spatio-temporal data observed on  $\mathcal{G}$  can be represented as a graph signal  $X \in \mathbb{R}^{N \times F}$ , where  $F$  is the number of features associated with each node. Let  $X^{(t)}$  denote the graph signal observed at time  $t$ . The spatio-temporal forecasting problem aims to learn a function  $\mathcal{F}(\cdot)$  that maps  $s$  historical graph signals to  $h$  future graph signals, given a graph  $\mathcal{G}$ :

$$[X^{(t-s+1)}, \dots, X^{(t)}; \mathcal{G}] \xrightarrow{\mathcal{F}(\cdot)} [X^{(t+1)}, \dots, X^{(t+h)}] \quad (1)$$

## 2.2 Related Work

**Spatio-temporal Forecasting.** Spatio-temporal forecasting has been studied for decades, aiming to predict future states by analyzing historical data. Traditional spatio-temporal prediction methods are mainly based on statistics and time series analysis, which have been successful to a certain extent, but have limitations in dealing with complex spatial structures and spatio-temporal relationships [28]. To address these issues, some models based on deep learning frameworks are effective in discovering potential feature representations such as non-linear spatial and temporal correlations from historical data [20]. Among these frameworks, Spatio-Temporal Graph Neural Networks (STGNNs) have become an emerging direction in prediction tasks. These models can better capture the spatio-temporal dynamics by integrating Graph Neural Networks (GNNs) [12] with temporal models [32]. Several STGNN models have been proposed in recent years, achieving remarkable results in spatio-temporal prediction tasks, such as Graph WaveNet [29], STGCN [31], DCRNN [13] and AGCRN [2]. Moreover, attention mechanism [27] has also become increasingly popular due to its effectiveness in modeling the dynamic dependencies in spatio-temporal data. Despite the diverse architecture of STGNN models, their performance improvements have reached a plateau [24], leading to a paradigm shift in research focus towards the integration of Self-Supervised Learning [24] and Large Language Models [33]. *Nonetheless, their enhancements in model performance are concomitant with the increasing model complexity. Underlying this, our approach proposes a novel approach concentrated on the node-specific predictor, aiming to augment existing STGNN methods by enhancing their efficiency with minimal increments in parameters and computational time.*

**Low Rank Matrix Factorization.** Low-rank matrix factorization aims to decompose a high-dimensional matrix, possibly containing noise, into the product of two or more low-rank matrices. This approach approximates the original matrix while minimizing information loss and reducing computational complexity. It finds wide applications in various fields such as natural language processing [3] and speech recognition [23]. LoRA [9], for instance, leverages the low intrinsic dimensionality of large language models to efficiently adapt them by injecting trainable low-rank matrices into each Transformer layer [1]. Similarly, in the context of Large Vocabulary Continuous Speech Recognition, low-rank matrix decomposition has been successfully applied to acoustic and language modeling [23]. Compacter [11] takes this approach a step further by incorporating task-specific weight matrices, low-rank optimization, and parameterized super-complex multiplication layers, which are efficiently computed using a shared "slow speedup" mechanism. In addition, the Low-rank matrix can also be utilized as adapter modules as demonstrated in the ST-Adapter [21] for cross-modality image-to-video transfer learning. By exploiting the inherent low-rank structure of weight matrices, these techniques significantly reduce the parameter count and computational complexity while maintaining model performance, demonstrating the immense potential of low-rank matrix factorization in optimizing deep

neural networks across a wide range of applications. Nonetheless, only a few studies have applied it to spatio-temporal forecasting. Specifically, MFSTN [22] or DeepLGN [16] utilize matrix or tensor factorization to decompose region-specific parameters into learnable matrices. *However, it relies on grid data modeling and focuses on predictions for specific regions, thus lacking generality. In contrast, our ST-LoRA, through carefully designed multi-layer node adapters, effectively models the heterogeneity of spatio-temporal node distributions.*

### 3 Methodology

In this section, we present ST-LoRA, a lightweight and efficient way to adjust the performance of spatio-temporal forecasting models. The overall architecture and core components of the model are shown in Figure 3.

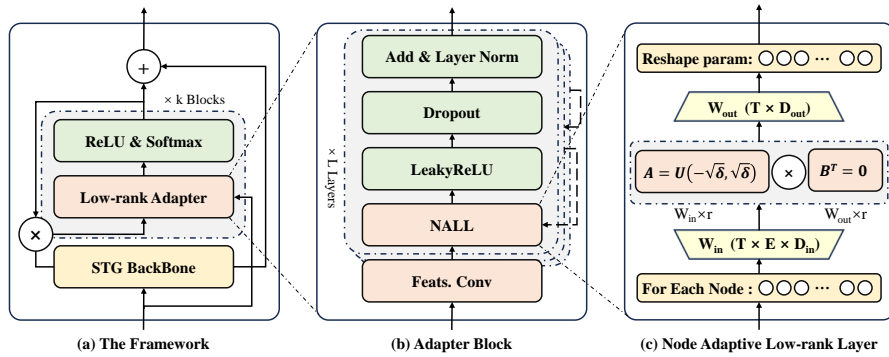


Fig. 3: Our proposed framework is shown in (a). And (b) is the computational process for one low-rank adapter block, as well as (c) is how we compute node-level weight adjustment using low-rank matrices.

#### 3.1 Node-Adaptive Low-rank Layers

A node adaptive low-rank layer (NALL) is a special kind of linear layer that adds extra low-rank matrices to tune the original parameter weight. We denoted the space as a matrix  $W = [w_1, \dots, w_n] \in \mathbb{R}^{N \times M}$ , where  $n$  is the number of nodes and  $N, M$  are the input and output dimensions of the model respectively. We are inspired by low-rank matrix decomposition that updating the parameter matrix can be computed from two low-rank matrices, which contain learnable additional parameters during training[14]. The NALL has a similar form as a fully-connected layer, which converts an input  $x \in \mathbb{R}^{T \times N \times d_i}$  to an output  $y \in \mathbb{R}^{T \times N \times d_o}$ . The formula for the update parameters is as follows:

$$y_i = \sigma(W^{(i)}x + \Delta W x + b), \quad \Delta W = B \times A \cdot \frac{\alpha}{r}, \quad (2)$$

where  $W^{(i)}$  denotes the extra parameter learned from NALLs for each node, and both  $A \in \mathbb{R}^{N \times r}$  and  $B \in \mathbb{R}^{r \times M}$  are learnable low-rank matrices, and the

factorized rank  $r << \min(N, M)$ . The number of training parameters is significantly reduced because we decompose the weight parameters into low-rank matrices A and B during transmission. In addition, we scale  $\Delta W$  by  $\frac{\alpha}{r}$ , which helps to minimize the need to readjust the hyper-parameters[9].

Due to the complexity and heterogeneity of spatio-temporal data, predictive models are usually very data-dependent. Spatio-temporal prediction models are hard to generalize, and fine-tuning for downstream tasks is particularly important. NALLs can improve the performance of the model by adding low-rank matrices which enable nodes to be adapted to specific scenarios, with only a very small number of parameters without increasing the complexity of the model[1].

During the forward and evaluation of NALLs, the output results are derived from the linear transformation of the original inputs, plus an adaptive extra parameter matrix obtained from the A and B computations. When training the pattern, the original weight matrix is subtracted from this multiplication of low-rank matrices. We iterate this process, with the result of each computed extra parameter requiring the use of a deflation factor to reduce the disturbances caused by a single adjustment, and then operations such as dropout, LeakyReLU, and normalization to simulate non-linear and complex patterns in the data. This process can be specifically expressed as follows:

---

**Algorithm 1** The process of node-level adjustment

---

**Input:** data X, shape  $[B, T, N, C]$   
 Predict using STG model  $\mathcal{F}(X) \rightarrow y_0 \in \mathbb{R}^{T \times N \times O}$   
 Denote  $AB$ =Adapter Blocks,  $LL$ =Low-rank Layers  
**for**  $i = 1$  **to**  $AB$  **do**  
 Initialize node embedding dimension size  $E = Ok$   
 Compress time series dimension  $w = TE$ .  
**for**  $j = 1$  **to**  $LL$  **do**  
 Initialize low-rank matrices A and B  
 Calculate  $\Delta W$  updates using low-rank matrices  
 $\Delta W + W_0 - > W_j$   
 $y_i^j = \mathcal{G}(y_i^{j-1}, \sigma(W_j))$   
**end for**  
 Reshape the weights back to the same tensor space as  $y_i$   
**end for**  
 Pool adjustment value  $\hat{y} = \mathcal{E}([y_1, \dots, y_k])$   
**Output:**  $y = \sum^{AB} \sum^{LL} (\mathcal{F} \cdot \sigma(\hat{y}))$

---

NALLs can improve the performance of the model because they introduce learnable parameters from low-rank matrices that can be well-trained to memorize and learn new data, including potential spatial and temporal information as well as spatio-temporal correlations[22]. This allows the model to capture complex patterns in the data, thus improving the accuracy of the predictions.

### 3.2 Multi-layer residual fusion module

Since the parameters of the model are learned during training, they may not be fully adapted to new or unseen data. To address this problem, We propose to

fit existing spatio-temporal forecasting models as the backbone with low-rank adapter blocks. The low-rank adapter internally employs a residual structure that learns the deep network using the parameter provided by the multi-layered node adaptive low-rank layer module, part of which is frozen parameters, making the training process more efficient. These additional parameters allow for fine-grained model tuning at each node to better accommodate new data.

This fusion module consists of multiple NALLs, each of which is a fully connected deep neural network layer that maps the input data into a new low-rank space to extract complex patterns in the data. The feature information of each time series of the node is encoded at the beginning by a convolution operation and multiple NALLs of the adapter are computed successively in the form of residuals, and activation functions and regularization terms are used in the computation process to control the model complexity, to prevent the module from overfitting and to enable the model parameters to simulate the complex spatio-temporal patterns. The formulation of ST-LoRA is defined as:

$$\hat{h}_t = \mathcal{H}^{(k)}(\sigma(\dots \mathcal{H}^{(1)}(\sigma(W))\dots)) \quad (3)$$

$$z_t = \frac{1}{b} \sum_{i=1}^b f_t \times \sigma(\hat{h}_i) \quad || \quad z_t = E(\hat{h}) \quad (4)$$

$$h_t = \mathcal{F}(X_{:t}) + z_t \quad (5)$$

where  $\sigma$  denotes the activation function, such as LeakyReLU,  $\mathcal{H}(\cdot)$  denotes the output of low-rank adapter blocks, and  $k$  denotes the number of layers. To make the effect of our method more stable, we would like to adjust the results several times using  $b$  adapter blocks and average pooling.

## 4 Experiment

In this section, we conduct extensive experiments to investigate the following Research Questions (RQ):

- **RQ1:** Can ST-LoRA be applied to a wide range of different deep spatio-temporal prediction models?
- **RQ2:** To what extent does our proposed method improve the performance of the original model?
- **RQ3:** How much extra time and parameters did we take to get these improvements?
- **RQ4:** How do different parameter settings lead to differences between experimental results?
- **RQ5:** Does our approach truly explain and alleviate node heterogeneity?

### 4.1 Experimental Setup

**1) Datasets:** Our approach is verified on six real-world datasets widely used in the field of spatio-temporal forecasting, each comprising tens of thousands of

time steps and hundreds of sensors. The statistical information for each dataset is summarized in Table 1. The first two datasets were proposed by DCRNN[13] and the last four datasets were proposed by STGCN [26]. The first two datasets focus on traffic speed, while the others capture traffic flow. The traffic speed data records the average vehicle speed (miles per hour), typically represented as a floating-point value usually less than 70, due to speed limits in the respective areas. On the other hand, traffic flow data is represented as integers, with values potentially reaching into the hundreds, reflecting the count of passing vehicles.

Table 1: Statistics and description of datasets we used.

Dataset	#Nodes	#Edges	#Frames	Time Range	Type
METR-LA	207	1515	34,272	03/01/2012 – 06/27/2012	Traffic speed
PEMS-BAY	325	2369	52,116	01/01/2017 – 06/30/2017	Traffic speed
PEMS03	358	547	26208	09/01/2018 – 11/30/2018	Traffic flow
PEMS04	307	340	16992	01/01/2018 – 02/28/2018	Traffic flow
PEMS07	883	866	28224	05/01/2017 – 08/06/2017	Traffic flow
PEMS08	170	295	17856	07/01/2016 – 08/31/2016	Traffic flow

All of the above datasets are divided along the time axis into three non-overlapping parts, including training, validation, and test sets. METR-LA and PEMS-BAY are divided in a fraction of 7:1:2 while PEMS03, PEMS04, PEMS07, and PEMS08 are divided in a fraction of 6:2:2.

**2) Evaluation Metrics:** The metrics we chose for evaluation include Mean Absolute Error (MAE), Root Mean Square Error (RMSE), and Mean Absolute Percentage Error (MAPE). Suppose  $x = x_1, \dots, x_n$  represents the ground truth,  $\hat{x} = \hat{x}_1, \dots, \hat{x}_n$  represents the predicted values, and  $\Omega$  denotes the indices of observed samples, the metrics are defined as follows.

$$MAE(x, \hat{x}) = \frac{1}{|\Omega|} \sum_{i \in \Omega} |x_i - \hat{x}_i| \quad (6)$$

$$RMSE(x, \hat{x}) = \sqrt{\frac{1}{|\Omega|} \sum_{i \in \Omega} (x_i - \hat{x}_i)^2} \quad (7)$$

$$MAPE(x, \hat{x}) = \frac{1}{|\Omega|} \sum_{i \in \Omega} \left| \frac{x_i - \hat{x}_i}{x_i} \right| \quad (8)$$

**3) Baselines:** We use the following classical spatio-temporal graph prediction models to compare the performance before and after the addition of our low-rank adapter:

- **LSTM.** Long Short-Term Memory network[8], a special RNN model that introduces a new gated mechanism to control the information flow by selectively retaining and forgetting temporal information in each time step.
- **STGCN.** Spatio-temporal graph convolution network[31], which combines graph convolution with 1D convolution.
- **GWNet.** Graph WaveNet[29], which uses an adaptive adjacency matrix to capture hidden spatial correlations in traffic data and 1D dilation convolution to capture temporal correlations.

- **AGCRN.** Adaptive Graph Convolutional Recurrent Network[2], which uses Node Adaptive Parameter Learning (NAPL) module and Data Adaptive Graph Generation (DAGG) module to automatically infer interdependencies between different flow time series.
- **D2STGNN.** The Decoupled Dynamic Spatio-Temporal Graph Neural Network[25], which can separate the diffusion and inherent traffic information, as well as decouple the hidden time series signals to improve dynamic graph learning capability.
- **STAE.** Spatio-Temporal Adaptive Embedding transformer [18], which uses a linear layer to extend feature dimension and then uses several embedding layers to separately encode features such as the node’s characteristics, spatial characteristics, and temporal characteristics.

**4) Implementation Details:** We implement the model with the PyTorch toolkit on a Linux server with NVIDIA GeForce RTX 2080 Ti GPUs. Adam is chosen as an optimizer with an initial learning rate of 0.001 and a weight decay of 0.0005 to train the model. Five fixed random seeds were used for each experiment, and the final experimental results were computed with mean and variance. We use the previous 12 time steps to predict the values on one feature channel in the next 12 time steps, as well as the average score of MAE, RMSE, and MAPE over 12 prediction horizons.

**5) Model Settings of ST-LoRA (RQ1)** We directly pass the baselines to the whole model as backbones without changing their original parameters. In the initialization of the model, the learning rate is set to be adjusted in step 10, and the ratio is 0.1. Various models are implemented concerning LargeST [19], a benchmark, and the official source code. For hyperparameters in the framework, such as the number of adapter blocks is usually taken as 1, the number of NALLs is usually taken as 4, and the maximum rank of the low-rank space is usually taken as 8, which is usually adjusted according to the original model. This setup ensures that we seamlessly integrate existing methods into our framework.

#### 4.2 Performance Comparisons (RQ2)

To prove that our proposed framework is effective, we first conduct repeated experiments using multiple models on all the above datasets. Specifically, here we give the boosting performance of each model on a single dataset as shown in Table 2, and the improvement of a single model on multiple datasets as shown in Table 3. For all datasets, we train and test each model at least five times and calculate the mean to get accurate results. For simplicity, the ST models enhanced by our proposed framework are named "base model+". We trained the spatio-temporal forecasting framework from scratch and compared performance between models with and without low-rank adapters, and the overwhelming results show that our method obtains lower loss compared to the original model and performs consistently on a variety of datasets and models.

Table 2: The improvement of different models in PEMS04 dataset. Here, lower values indicate better performance.

Model	60min			Average		
	MAE ↓	RMSE ↓	MAPE ↓	MAE ↓	RMSE ↓	MAPE ↓
HI	42.37	61.67	29.96	42.36	61.66	29.92%
VAR	26.76	40.28	20.94	23.51	36.39	17.85%
SVR	37.86	56.01	26.72	28.66	44.59	19.15%
LSTM	26.73	41.75	18.47%	22.43	35.39	15.32%
LSTM+	26.46	41.44	18.27%	22.26	35.21	15.25%
$\Delta$	-0.27	-0.31	-0.20%	-0.17	-0.18	-0.07%
STGCN	22.34	34.89	15.87%	20.67	32.29	14.86%
STGCN+	22.07	34.47	15.42%	20.37	31.94	14.36%
$\Delta$	-0.27	-0.43	-0.45%	-0.30	-0.35	-0.50%
GWNet	22.05	34.28	15.89%	19.88	31.37	13.96%
GWNet+	21.21	33.33	15.27%	19.35	30.74	13.81%
$\Delta$	-0.84	-0.95	-0.62%	-0.54	-0.64	-0.15%
AGCRN	20.30	32.97	14.32%	19.03	30.95	13.35%
AGCRN+	20.16	32.65	14.30%	18.94	30.71	13.30%
$\Delta$	-0.14	-0.32	-0.02%	-0.09	-0.24	-0.05%
STAE	20.59	32.71	14.79%	19.02	30.45	13.44%
STAE+	20.40	32.38	15.00%	18.89	30.22	13.58%
$\Delta$	-0.19	-0.33	0.21%	-0.12	-0.23	0.14%
D2STGNN	23.34	35.89	17.39%	20.75	32.36	15.91%
D2STGNN+	23.36	35.64	17.16%	20.62	32.16	14.95%
$\Delta$	0.01	-0.24	-0.23%	-0.13	-0.20	-0.96%

From Table 2, both the classical spatio-temporal forecasting models like STGCN and the SOTA models like STAEFormer are almost always able to get a stable performance when trained from scratch in combination with our framework. However, we observe limited improvement on methods like D2STGNN, specifically a slight rise in the MAE metric at the long 60-minute time step. We believe that two reasons exist. One is that the model itself is sufficiently complex that our adapter does not explain and cooperate well with the original model during computation. The second is that the added parameter space of the low-rank matrices does not sufficiently adjust the weights of each dimension to capture both long- and short-term dependencies evenly. Nevertheless, there is an across-the-board boost in the average time step. Throughout Table 2 the models achieve an average of 0.3 MAE drop, especially Graph-WaveNet on the PEMS04 dataset which significantly gets 0.54 average MAE drop. It shows that the framework helps the model to enhance the generalization ability.

They performed better because in the case that the prediction results of the backbone can be close to the real value, our method can additionally provide enough adjustment space to guarantee the fitting results, which are thanks to the low-rank matrix factorization technique helping us to spend less computational resources to improve the hidden dimensions of all nodes. Specifically, the

Table 3: The improvement of one model in different datasets. STGCN is taken as a reference here.

Datasets	Model	60min			Average		
		MAE ↓	RMSE ↓	MAPE ↓	MAE ↓	RMSE ↓	MAPE ↓
PEMS04	STGCN	22.34	34.89	15.87%	20.67	32.29	14.86%
	STGCN+	22.07	34.47	15.42%	20.37	31.94	14.36%
	Δ	-0.27	-0.43	-0.45%	-0.30	-0.35	-0.50%
PEMS08	STGCN	18.23	28.29	12.41%	16.65	25.64	11.55%
	STGCN+	17.83	27.85	12.06%	16.38	25.42	11.18%
	Δ	-0.40	-0.44	-0.35%	-0.27	-0.22	-0.37%
PEMS03	STGCN	19.29	32.09	20.12%	17.17	28.68	18.38%
	STGCN+	18.84	31.74	18.87%	16.85	28.33	17.50%
	Δ	-0.45	-0.35	-1.25%	-0.32	-0.35	-0.88%
PEMS07	STGCN	27.09	41.85	12.21%	24.26	37.33	11.14%
	STGCN+	26.50	41.26	11.89%	23.90	36.96	10.94%
	Δ	-0.59	-0.59	-0.32%	-0.37	-0.36	-0.20%
METR-LA	STGCN	3.58	7.47	10.46%	3.13	6.29	8.68%
	STGCN+	3.54	7.43	10.40%	3.10	6.26	8.63%
	Δ	-0.04	-0.04	-0.06%	-0.03	-0.04	-0.05%
PEMSBAY	STGCN	2.04	4.61	4.81%	1.68	3.66	3.83%
	STGCN+	1.99	4.53	4.73%	1.64	3.59	3.74%
	Δ	-0.05	-0.08	-0.08%	-0.04	-0.06	-0.09%

additional parameters provided by the low-rank matrices can incorporate more complex spatio-temporal dependencies, let's say for features in a region, features at different periods, or relationships between neighboring points as well as features at adjacent time steps, which can be better computed with a compressed number of parameters.

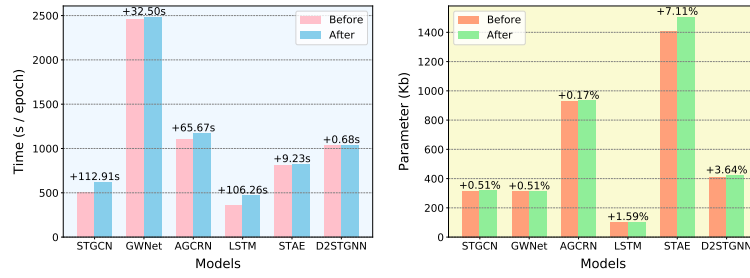
Based on the same principle, the results in Table 3 show the performance of STGCN is improved on all six datasets, which indicates that our proposed method has generalization ability itself and is better able to deal with spatio-temporal data with larger scale and more complex spatio-temporal dependencies.

### 4.3 Efficiency and scalability Studies (RQ3)

**Time Efficiency.** In Figure 4(a), we show the difference in time cost between training some models from scratch before and after using our proposed adapter. We fixed the addition of 16 node adaptive low-rank layers and set the embedding dimension to 32 to experiment. We find that the low-rank portion of our framework allows training time to remain stable even when multiple Low-rank Adapters are used and to get lower performance.

**Framework Scalability.** We experiment with a fixed number of node adaptive low-rank layers and six different baselines in the overall framework. As shown in Figure 4(b), except STAE, all models are added less than 4% of the total parameters, yet they can drop the metrics by as much as 5%. This shows that

our proposed framework is lightweight and efficient, although when the backbone model is large or computational resources are limited.



(a) Processing time for PEMSBAY. (b) Training parameter Added.

Fig. 4: Efficiency Study.

#### 4.4 Parameter Sensitivity Analysis (RQ4)

In our experiments, we fixed the number of layers to be 4, as well as the node embedding dimension to be 12, which are the two most critical parameters. The node embedding dimension represents the rank of the low-rank matrix required for the extra parameter space of the nodes, which tends to increase as more feature information is included in the data. And after stacking multiple layers of NALL, the fine-tuning effect of these extra parameter spaces can be amplified. It is important to design these two hyper-parameters in a balanced way because a larger parameter space does not mean easier to learn. We again use the STGCN model and the PEM04 dataset as an example to explore the relationship between the size of this dataset as well as the two hyperparameters and the lifting effect, and the results are shown in Figure 5.

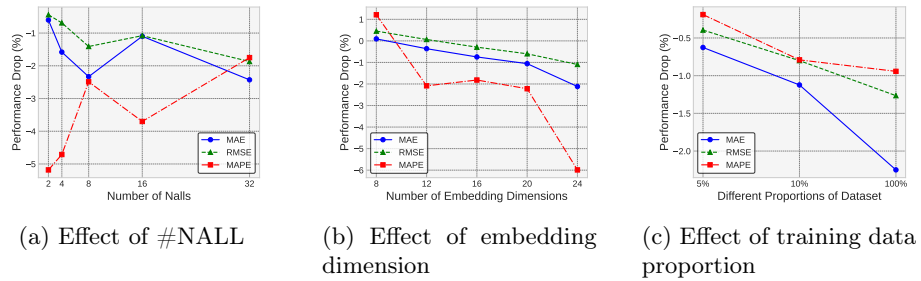


Fig. 5: Parameter Study.

#### 4.5 Visualization Case Study (RQ5)

To further explore why the embeddings obtained by our proposed LAST framework can deliver more accurate traffic prediction than the original model, we

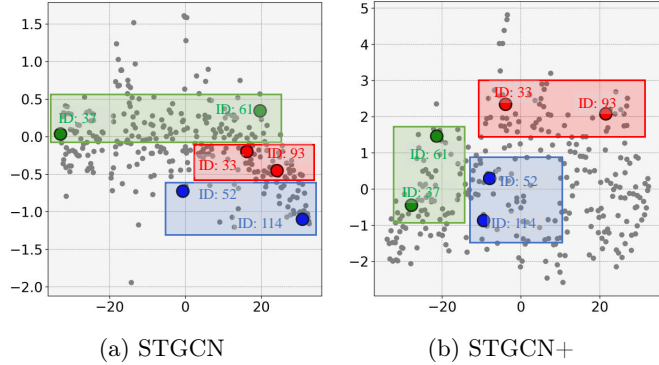


Fig. 6: t-SNE visualization of embeddings on PMES04.

investigate the case of STGCN as applied to the PEMS04 dataset. Specifically, we employ t-SNE to visualize the embeddings obtained by both the original STGCN and the LAST-augmented STGCN (STGCN+). We proceed to plot the final prediction outcomes for all nodes under consideration. As depicted in Figure 6, it is evident that the samples belonging to the same category exhibit a higher degree of compactness in the visualization results of STGCN+, in contrast to those obtained from STGCN. Specifically, the original model yields a dense range of node representations, but the three pairs of observation nodes are not closer two by two, suggesting that the positional relationships among nodes are not well learned; whereas our approach allows all point predictions to be more dispersed and the same species to be closer to each other, suggesting that a low-rank matrix factorization facilitates the learning of complex relationships between nodes. Such a mechanism is instrumental in enhancing the accuracy of traffic predictions.

## 5 Conclusion

In this paper, we focus on challenges such as spatio-temporal heterogeneity and weak node generalization capability in spatio-temporal modeling. We introduce a node-level adaptation framework, namely ST-LoRA, leveraging residual fusion modules with node-adaptive low-rank layers. Our proposed approach enhances existing models, effectively capturing heterogeneous characteristics and distribution variations within independent nodes. Given that the current framework is only utilized for adapting paradigms trained from scratch, in future work, we aim to further explore fine-tuning stages and more universally applicable adapter structures to address the transfer and generalization capabilities of spatio-temporal representations across different datasets.

## References

1. Aghajanyan, A., Zettlemoyer, L., Gupta, S.: Intrinsic dimensionality explains the effectiveness of language model fine-tuning. arXiv preprint arXiv:2012.13255 (2020)

2. Bai, L., Yao, L., Li, C., Wang, X., Wang, C.: Adaptive graph convolutional recurrent network for traffic forecasting. *Advances in neural information processing systems* **33**, 17804–17815 (2020)
3. Bouchard, G., Naradowsky, J., Riedel, S., Rocktäschel, T., Vlachos, A.: Matrix and tensor factorization methods for natural language processing. In: *Proceedings of the 53rd Annual Meeting of the Association for Computational Linguistics and the 7th International Joint Conference on Natural Language Processing: Tutorial Abstracts*. pp. 16–18 (2015)
4. Box, G.E., Pierce, D.A.: Distribution of residual autocorrelations in autoregressive-integrated moving average time series models. *Journal of the American statistical Association* **65**(332), 1509–1526 (1970)
5. Chen, C., Petty, K., Skabardonis, A., Varaiya, P., Jia, Z.: Freeway performance measurement system: mining loop detector data. *Transportation Research Record* **1748**(1), 96–102 (2001)
6. Chung, J., Gulcehre, C., Cho, K., Bengio, Y.: Empirical evaluation of gated recurrent neural networks on sequence modeling. *arXiv preprint arXiv:1412.3555* (2014)
7. Du, R., Santi, P., Xiao, M., Vasilakos, A.V., Fischione, C.: The sensible city: A survey on the deployment and management for smart city monitoring. *IEEE Communications Surveys & Tutorials* **21**(2), 1533–1560 (2018)
8. Hochreiter, S., Schmidhuber, J.: Long short-term memory. *Neural computation* **9**(8), 1735–1780 (1997)
9. Hu, E.J., Shen, Y., Wallis, P., Allen-Zhu, Z., Li, Y., Wang, S., Wang, L., Chen, W.: Lora: Low-rank adaptation of large language models. *arXiv preprint arXiv:2106.09685* (2021)
10. Jin, G., Liang, Y., Fang, Y., Shao, Z., Huang, J., Zhang, J., Zheng, Y.: Spatio-temporal graph neural networks for predictive learning in urban computing: A survey. *IEEE Transactions on Knowledge and Data Engineering* (2023)
11. Karimi Mahabadi, R., Henderson, J., Ruder, S.: Compacter: Efficient low-rank hypercomplex adapter layers. *Advances in Neural Information Processing Systems* **34**, 1022–1035 (2021)
12. Kipf, T.N., Welling, M.: Semi-supervised classification with graph convolutional networks. *arXiv preprint arXiv:1609.02907* (2016)
13. Li, Y., Yu, R., Shahabi, C., Liu, Y.: Diffusion convolutional recurrent neural network: Data-driven traffic forecasting. *arXiv preprint arXiv:1707.01926* (2017)
14. Li, Y., Ma, T., Zhang, H.: Algorithmic regularization in over-parameterized matrix sensing and neural networks with quadratic activations. In: *Conference On Learning Theory*. pp. 2–47. PMLR (2018)
15. Liang, Y., Ke, S., Zhang, J., Yi, X., Zheng, Y.: Geoman: Multi-level attention networks for geo-sensory time series prediction. In: *IJCAI*. vol. 2018, pp. 3428–3434 (2018)
16. Liang, Y., Ouyang, K., Wang, Y., Liu, Y., Zhang, J., Zheng, Y., Rosenblum, D.S.: Revisiting convolutional neural networks for citywide crowd flow analytics. In: *Machine Learning and Knowledge Discovery in Databases: European Conference, ECML PKDD 2020, Ghent, Belgium, September 14–18, 2020, Proceedings, Part I*. pp. 578–594. Springer (2021)
17. Liang, Y., Xia, Y., Ke, S., Wang, Y., Wen, Q., Zhang, J., Zheng, Y., Zimmermann, R.: Airformer: Predicting nationwide air quality in china with transformers. In: *Proceedings of the AAAI Conference on Artificial Intelligence*. pp. 14329–14337 (2023)

18. Liu, H., Dong, Z., Jiang, R., Deng, J., Deng, J., Chen, Q., Song, X.: Spatio-temporal adaptive embedding makes vanilla transformer sota for traffic forecasting. In: Proceedings of the 32nd ACM international conference on information and knowledge management. pp. 4125–4129 (2023)
19. Liu, X., Xia, Y., Liang, Y., Hu, J., Wang, Y., Bai, L., Huang, C., Liu, Z., Hooi, B., Zimmermann, R.: Largest: A benchmark dataset for large-scale traffic forecasting. *Advances in Neural Information Processing Systems* **36** (2024)
20. Lv, Y., Duan, Y., Kang, W., Li, Z., Wang, F.Y.: Traffic flow prediction with big data: A deep learning approach. *IEEE Transactions on Intelligent Transportation Systems* **16**(2), 865–873 (2014)
21. Pan, J., Lin, Z., Zhu, X., Shao, J., Li, H.: St-adapter: Parameter-efficient image-to-video transfer learning. *Advances in Neural Information Processing Systems* **35**, 26462–26477 (2022)
22. Pan, Z., Wang, Z., Wang, W., Yu, Y., Zhang, J., Zheng, Y.: Matrix factorization for spatio-temporal neural networks with applications to urban flow prediction. In: Proceedings of the 28th ACM international conference on information and knowledge management. pp. 2683–2691 (2019)
23. Sainath, T.N., Kingsbury, B., Sindhwan, V., Arisoy, E., Ramabhadran, B.: Low-rank matrix factorization for deep neural network training with high-dimensional output targets. In: 2013 IEEE international conference on acoustics, speech and signal processing. pp. 6655–6659. IEEE (2013)
24. Shao, Z., Zhang, Z., Wang, F., Xu, Y.: Pre-training enhanced spatial-temporal graph neural network for multivariate time series forecasting. In: Proceedings of the 28th ACM SIGKDD Conference on Knowledge Discovery and Data Mining. pp. 1567–1577 (2022)
25. Shao, Z., Zhang, Z., Wei, W., Wang, F., Xu, Y., Cao, X., Jensen, C.S.: Decoupled dynamic spatial-temporal graph neural network for traffic forecasting. *arXiv preprint arXiv:2206.09112* (2022)
26. Song, C., Lin, Y., Guo, S., Wan, H.: Spatial-temporal synchronous graph convolutional networks: A new framework for spatial-temporal network data forecasting. In: Proceedings of the AAAI conference on artificial intelligence. pp. 914–921 (2020)
27. Vaswani, A., Shazeer, N., Parmar, N., Uszkoreit, J., Jones, L., Gomez, A.N., Kaiser, L., Polosukhin, I.: Attention is all you need. *Advances in neural information processing systems* **30** (2017)
28. Wang, X., Ma, Y., Wang, Y., Jin, W., Wang, X., Tang, J., Jia, C., Yu, J.: Traffic flow prediction via spatial temporal graph neural network. In: Proceedings of the web conference 2020. pp. 1082–1092 (2020)
29. Wu, Z., Pan, S., Long, G., Jiang, J., Zhang, C.: Graph wavenet for deep spatial-temporal graph modeling. *arXiv preprint arXiv:1906.00121* (2019)
30. Yao, H., Wu, F., Ke, J., Tang, X., Jia, Y., Lu, S., Gong, P., Ye, J., Li, Z.: Deep multi-view spatial-temporal network for taxi demand prediction. In: Proceedings of the AAAI conference on artificial intelligence (2018)
31. Yu, B., Yin, H., Zhu, Z.: Spatio-temporal graph convolutional networks: A deep learning framework for traffic forecasting. *arXiv preprint arXiv:1709.04875* (2017)
32. Yu, Y., Si, X., Hu, C., Zhang, J.: A review of recurrent neural networks: Lstm cells and network architectures. *Neural computation* **31**(7), 1235–1270 (2019)
33. Zhou, T., Niu, P., Sun, L., Jin, R., et al.: One fits all: Power general time series analysis by pretrained lm. *Advances in neural information processing systems* **36** (2024)
34. Zivot, E., Wang, J.: Vector autoregressive models for multivariate time series. Modeling financial time series with S-PLUS® pp. 385–429 (2006)